The Influence of Specific Activity on the Biodistribution of ^{18}F-rhPSMA-7.3: A Retrospective Analysis of Clinical PET Data

Thomas Langbein[1], Alexander Wurzer[2], Andrei Gafita[1,3], Andrew Robertson[1], Hui Wang[1], Ayça Arçay[1,4], Michael Herz[1], Hans-Juergen Wester[2], Wolfgang A. Weber[1], and Matthias Eiber[1]

[1]*Department of Nuclear Medicine, Klinikum rechts der Isar, School of Medicine, Technical University of Munich, Munich, Germany;* [2]*Chair of Pharmaceutical Radiochemistry, Technical University of Munich, Garching, Germany;* [3]*Ahmanson Translational Theranostics Division, Department of Molecular and Medical Pharmacology, UCLA, Los Angeles, California; and* [4]*Department of Nuclear Medicine, Akdeniz University, Antalya, Turkey*

We investigated whether the time between synthesis and injection and the resulting decrease in specific activity affects the normal-organ and tumor uptake of the PSMA ligand ^{18}F-rhPSMA-7.3 in patients with prostate cancer. **Methods:** The biodistribution of ^{18}F-rhPSMA-7.3 on PET/CT scans obtained with a high specific activity (median, 178.9 MBq/μg; $n = 42$) and a low specific activity (median, 19.3 MBq/μg; $n = 42$) was compared. **Results:** Tracer uptake by the parotid gland, submandibular gland, and spleen was moderately but significantly lower in the low-specific-activity group than in the high-specific-activity group (median SUV_{mean}, 16.7 vs. 19.2; 18.1 vs. 22.3; and 7.8 vs. 9.6, respectively). No other statistically significant differences were found for normal organs or tumor lesions. **Conclusion:** A 10-fold decrease in specific activity has only minor effects on the biodistribution of ^{18}F-rhPSMA-7.3. These findings suggest that ^{18}F-labeled PSMA ligands can be centrally produced and shipped to PET clinics in a similar way to ^{18}F-FDG.

Key Words: PSMA; PET/CT; biodistribution; molar activity; ^{18}F

J Nucl Med 2022; 63:742–745
DOI: 10.2967/jnumed.121.262471

Several ^{18}F-labeled prostate-specific membrane antigen (PSMA) ligands are currently in clinical development for imaging of patients with prostate cancer (*1–3*). In the future, it is envisioned that these ligands will be produced by central radiopharmacies in batch sizes similar to ^{18}F-FDG and shipped to PET clinics. In such a setting, radioactive decay will lead to a continuous decrease in the specific activity of the PSMA ligands. This decrease in specific activity could, in principle, lead to lower tumor uptake, since the ^{18}F-labeled PSMA ligands compete with the nonlabeled PSMA ligands for binding to the limited number of PSMA molecules. Such a saturation of tracer uptake by a nonradioactive precursor does not occur for ^{18}F-FDG because ^{18}F-FDG follows the flow of glucose, which is present at concentrations that are orders of magnitude higher.

^{18}F-rhPSMA-7.3 represents the lead compound in a class of radiohybrid PSMA (rhPSMA) ligands that can be labeled with ^{18}F for imaging but also with radiometals for therapeutic use (*4*). ^{18}F-rhPSMA-7.3 is a single diastereoisomer form of ^{18}F-rhPSMA-7, for which promising preliminary imaging data have been reported (*5,6*). Two multicenter, phase III trials are in progress to investigate the diagnostic accuracy of ^{18}F-rhPSMA-7.3 in primary staging (NCT04186819) and recurrence (NCT04186845) of prostate cancer.

Preclinical investigations have shown that the biodistribution of ^{18}F-labeled PSMA ligands in mice is significantly affected by the specific activity, with decreased uptake in tumor lesions and salivary glands at lower specific activities (*7*). The present study explored whether such effects also occur in humans over the range of specific activities typically injected for PSMA PET/CT studies.

MATERIALS AND METHODS

Study Design

We retrospectively reviewed data from patients who underwent ^{18}F-rhPSMA-7.3 PET/CT at our institution between August 2018 and October 2019 (Supplemental Fig. 1; supplemental materials are available at http://jnm.snmjournals.org). All reported investigations were conducted in accordance with the Helsinki Declaration and with national regulations. The retrospective analysis was approved by the Ethics Committee of the Technical University Munich (permit 290/18S), and the requirement to obtain informed consent was waived. ^{18}F-rhPSMA-7.3 administration complied with the German Medicinal Products Act, Arzneimittelgesetz §13 2b, and the responsible regulatory body (Government of Oberbayern).

^{18}F-rhPSMA-7.3 Synthesis, Administration, and Image Acquisition

^{18}F-rhPSMA-7.3 was synthesized as recently reported (*4*) and administered as an intravenous bolus (median, 321 MBq; interquartile range [IQR], 290–360 MBq) at a median of 71 min (IQR, 66–79 min) before the PET/CT scan began. Patients underwent ^{18}F-rhPSMA-7.3 PET/CT on a Biograph mCT flow scanner (Siemens Medical Solutions) as recently described (*5,6*).

Patient Selection

The patients had received the injection of ^{18}F-rhPSMA-7.3 at various time points after production and, consequently, had been administered

Received Apr. 25, 2021; revision accepted Aug. 5, 2021.
For correspondence or reprints, contact Thomas Langbein (thomas.langbein@tum.de).
Guest Editor: Ken Herrmann, Universitätsklinikum Essen
Published online Aug. 12, 2021.

different specific activities of ^{18}F-rhPSMA-7.3. The specific activity at the time of tracer injection was calculated for every patient using the exact time of injection, the injected activity, and the radiolabeling quality control data for the particular batch, while accounting for the known radioactive decay of ^{18}F. Two patient groups were created (high or low specific activity), aiming for a 10-fold difference between groups. In addition, groups were matched for uptake time and body weight, and only patients with a low tumor load were included to avoid tumor sink effects. A low tumor load was defined as no more than 1% of total injected dose accumulated in tumor lesions determined by isocontour volume-of-interest measurements at 50% of the SUV_{max}.

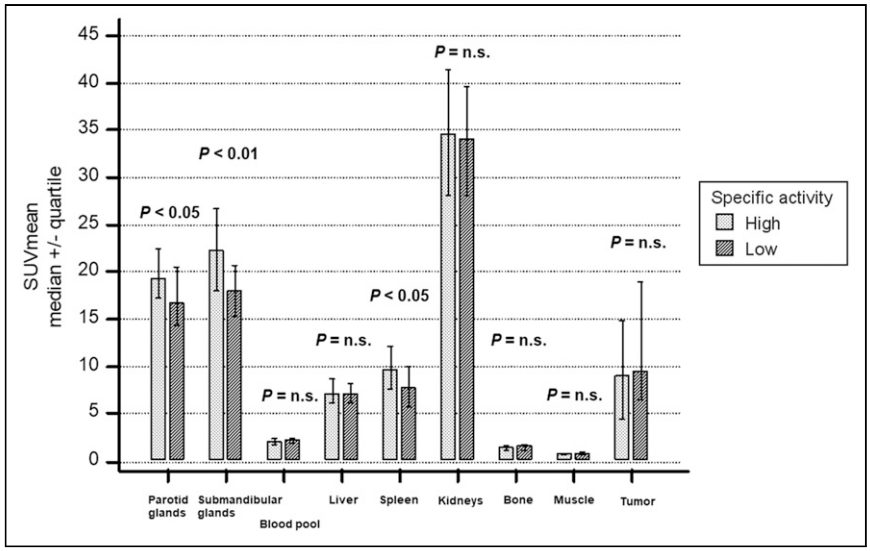

FIGURE 1. ^{18}F-rhPSMA-7.3 SUV_{mean} stratified by injected specific activity. n.s. = not statistically significant.

Biodistribution Assessment

SUV_{mean} was determined within standardized isocontour volumes of interest with 50% of the SUV_{max} and a diameter of 30 mm (salivary glands, liver, spleen, kidneys, bone, muscle, blood pool, and tumor lesions). For evaluation of the tumor uptake, volumes of interest were placed over a maximum of 3 lesions per patient in decreasing order of the SUV_{max}, and SUV_{mean} was averaged. The image-derived whole-organ radioactivity concentration (kBq/mL) based on full-organ segmentation (salivary glands, liver, spleen, and kidneys) was determined using semiautomatic analysis with the software qPSMA as previously described (*8*). Volume-of-interest placement and image analyses were performed by 2 experienced nuclear medicine physicians.

Statistical Analysis

The Mann–Whitney *U* test was used to test for differences between uptake parameters between the high- and the low-specific-activity groups. Additionally, a 1-way multivariate AVOVA was performed to analyze the effect of specific activities on biodistribution. Normal distribution of variables was evaluated by Q–Q plots and the Shapiro–Wilk W test. Data are presented as median and IQR; a *P* value of less than 0.05 was considered statistically significant. Statistical analysis was performed with SPSS Statistics, version 24 (IBM Corp.), and MedCalc, version 14.8.1 (MedCalc Software Ltd.).

RESULTS

Patient Population

From a total of 1,975 patients, 84 were selected and stratified into 2 groups of equal size. The median interval between tracer synthesis and injection was 72 min (IQR, 54–89 min) versus 367 min (IQR, 342–397 min) for the high and low groups ($P < 0.001$), resulting in a median specific activity of 178.9 MBq/μg (IQR, 158.6–199.1 MBq/μg) and 19.3 MBq/μg (IQR, 17.7–22.5 MBq/μg), respectively, for ^{18}F-rhPSMA-7.3 ($P < 0.001$). Median injected activity per kilogram of body weight (4.0 MBq/kg [IQR, 3.9–4.0 MBq/kg] vs. 4.0 MBq/kg [IQR, 3.9–4.0 MBq/kg]) and median ^{18}F-rhPSMA-7.3 uptake time (70 min [IQR, 65–76 min] vs. 75 min [IQR, 68–87 min]) were similar in the high and low groups ($P = 0.62$ and 0.06, respectively). No substantial differences between the groups were present for any clinical parameter (Supplemental Table 1). Supplemental Table 2 provides data for specific activities at calibration and injection.

Normal-Organ Biodistribution and Tumor Lesions Evaluated by SUV_{mean}

Median SUV_{mean} in the low-specific-activity group was significantly lower for parotid glands ($P = 0.014$), submandibular glands ($P = 0.002$), and spleen ($P = 0.012$) (Fig. 1; Supplemental Table 3). No significant differences in SUV_{mean} were found for the other investigated organs. Median SUV_{mean} was 9.0 (IQR, 4.4–14.8) and

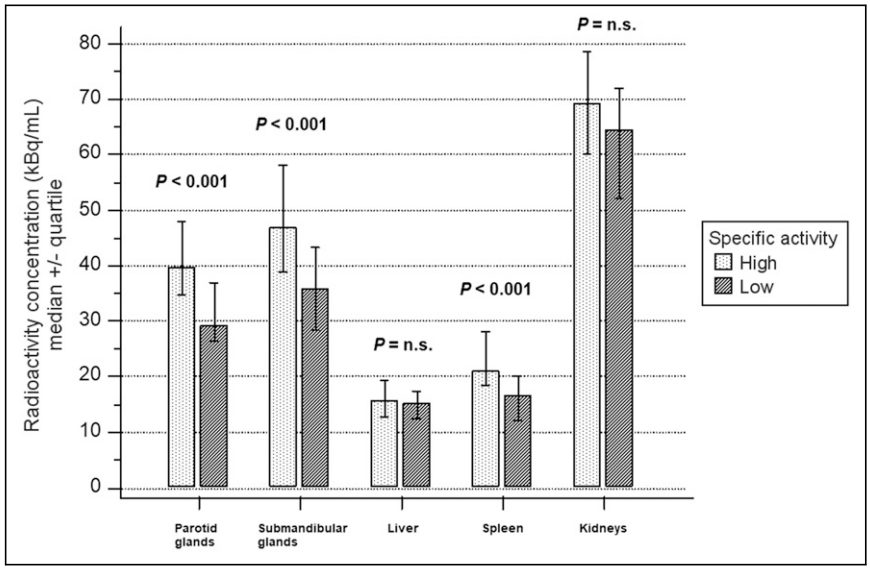

FIGURE 2. ^{18}F-rhPSMA-7.3 whole-organ radioactivity concentration stratified by injected specific activity. n.s. = not statistically significant.

9.5 (IQR, 6.5–19.0) for tumor lesions in the high- versus low-specific-activity groups, respectively, and not significantly different ($P = 0.273$). No statistical difference in tumor lesion distribution was observed between the 2 groups (Supplemental Fig. 2).

Whole-Organ Radioactivity Concentrations

Whole-organ radioactivity concentrations (kBq/mL) for the high- versus low-specific-activity groups were 39.6 (IQR, 34.8–48.0) versus 29.4 (IQR, 26.5–37.0), 46.9 (IQR, 38.9–58.1) versus 35.8 (IQR, 28.6–43.2), 15.7 (IQR, 12.6–19.4) versus 15.1 (IQR, 12.4– 17.5), 21.1 (IQR, 18.4–28.1) versus 16.5 (IQR, 12.2–20.0), and 69.3 (IQR, 60.0–78.6) versus 64.6 (IQR, 52.1–72.1) for the parotid glands, submandibular glands, liver, spleen, and kidneys, respectively. Results for the low-specific-activity group were significantly lower for salivary glands and spleen (each $P < 0.001$), whereas liver and kidneys did not show significant differences (Fig. 2).

A 1-way multivariate ANOVA confirmed the statistically significant difference between the high- and low-specific-activity groups for tracer distribution determined by SUV_{mean} and full-organ segmentation (combined dependent variables, $F_{14,60} = 3.928$, $P < 0.001$, partial $\eta^2 = 0.478$, Wilks $\Lambda = 0.522$.)

DISCUSSION

In this retrospective analysis, we explored the impact of ^{18}F-rhPSMA-7.3 specific activity on biodistribution in normal organs and tumors. Our data show that uptake patterns in organs relevant to clinical imaging interpretation are not substantially affected by different specific activities, with only the salivary glands and spleen demonstrating a moderate, albeit significant, decrease in the low- compared with high-specific-activity groups. Tumor uptake appeared stable over the 10-fold difference investigated. Our results indicate that clinical PET interpretation is not affected using a single large-batch production over several hours during the workday and the resultant wide range of injected specific activities.

Similar effects have already been demonstrated by Soeda et al. in a preclinical setting (*7*). In a mouse xenograft model derived from human lymph node metastases, a substantial decline in the SUV_{mean} of tumor lesions and salivary glands was observed on ^{18}F-PSMA-1007 PET/CT when the molar activity was reduced over a 100-fold range (*7*). Despite decreased tumor uptake, the tumor–to–salivary gland ratio increased as salivary gland uptake was even further reduced compared with tumors. The authors concluded that the increased tumor–to–salivary gland ratio might play a role in reducing off-target uptake of PSMA-targeting radioligand therapies. Comparable findings have been demonstrated with ^{68}Ga-labeled PSMA inhibitors using triazacyclononane-triphosphinate chelators (*9*). By the addition of unlabeled compounds, the accumulation was altered significantly in the kidneys and salivary glands but less so in the tumor, with a more beneficial kidney-to-tumor ratio in lower molar activities of 8 versus 1,200 MBq/nmol (*9*).

To translate these animal data into a clinical context, 2 different methodologies for detection of imaging-derived biodistribution of ^{18}F-rhPSMA-7.3 were applied. Recently, the biodistribution of ^{18}F-rhPSMA-7.3 was investigated in 6 healthy subjects, with ^{18}F-rhPSMA-7.3 showing high physiologic uptake in the kidneys and salivary glands (*10*). Our study demonstrated that uptake by most organs is not influenced by administration of lower specific activities, as might occur in a busy PET clinic. This consistency of uptake appears essential for a clinical PET/CT reading. Additionally, tumor uptake did not vary significantly, even with a 10-fold difference in the injected specific activity.

This difference in specific activity represents the realistic spectrum of what is observed in a real-world scenario for PET imaging. Although some of the mentioned preclinical findings could also be observed in our investigation with significant effect, they appeared to be without clinical relevance in the case of salivary gland and spleen uptake. Notably, because therapeutic applications usually require higher molar masses (~50–200 μg), our data cannot be extrapolated to the potential therapeutic use of rhPSMA-7.3.

The results of our study indicate that salivary gland uptake is saturable, suggesting binding to a target protein within the salivary glands. Similar findings were shown in preclinical studies of ^{177}Lu-PSMA-617, for which uptake in the salivary glands and kidneys of PC3-PIP tumor–bearing mice significantly declined without an impact on tumor uptake when cold PSMA-11 was added (*11*).

Some limitations of our study should be considered, for example, the retrospective design. However, we believe that our observations are true reflections of the variance in specific activity in daily clinical practice. Second, our cohort comprised a relatively heterogeneous patient group at different stages of prostate cancer. Nevertheless, we tried to control for any potential influence on biodistribution, selecting patients on the basis of a low tumor load. The heterogeneous population and the known high variance of in vivo PSMA expression might explain the wide range of reported SUV_{mean} in tumor lesions.

In summary, our data suggest that a single production of ^{18}F-rhPSMA-7.3 can be used in a clinical setting throughout the whole working day without a clinically relevant effect on biodistribution, especially tumor lesion uptake, despite a significantly decreasing specific activity. This observation underlines the potential logistical and economic advantages of ^{18}F-labeled PSMA ligands resulting from a single large-batch production in a cyclotron facility over generator-produced ^{68}Ga-based ligands with a short half-life and the need for multiple batches throughout the day (*12*).

CONCLUSION

Differences in the injected specific activity of ^{18}F-rhPSMA-7.3 observed throughout a usual working day have no clinically relevant effect on biodistribution and, especially, uptake by tumor lesions. These results support central production of ^{18}F-labeled PSMA ligands with shipment to PET clinics, similarly to ^{18}F-FDG.

DISCLOSURE

There is a patent application for rhPSMA (Matthias Eiber, Alexander Wurzer, and Hans-Juergen Wester). Matthias Eiber and Wolfgang Weber are consultants for Blue Earth Diagnostics (licensee for rhPSMA). No other potential conflict of interest relevant to this article was reported.

ACKNOWLEDGMENT

Editorial support was provided by Dr. Catriona Turnbull (Blue Earth Diagnostics).

KEY POINTS

QUESTION: Does the specific activity of the radiopharmaceutical administered to a patient affect the way it is distributed among organs?

PERTINENT FINDINGS: This retrospective data review showed that although the salivary glands and spleen appear to be saturable with decreasing specific activities, there was no clinically meaningful difference in organ uptake in patients with prostate cancer.

IMPLICATIONS FOR PATIENT CARE: A single batch of ^{18}F-rhPSMA-7.3 can be used throughout the day to scan multiple patients, with no effect on image quality being observed between the first and last patients of the day.

REFERENCES

1. Dietlein M, Kobe C, Kuhnert G, et al. Comparison of [^{18}F]DCFPyL and [^{68}Ga]Ga-PSMA-HBED-CC for PSMA-PET imaging in patients with relapsed prostate cancer. *Mol Imaging Biol.* 2015;17:575–584.
2. Giesel FL, Hadaschik B, Cardinale J, et al. F-18 labelled PSMA-1007: biodistribution, radiation dosimetry and histopathological validation of tumor lesions in prostate cancer patients. *Eur J Nucl Med Mol Imaging.* 2017;44:678–688.
3. Werner RA, Derlin T, Lapa C, et al. ^{18}F-labeled, PSMA-targeted radiotracers: leveraging the advantages of radiofluorination for prostate cancer molecular imaging. *Theranostics.* 2020;10:1–16.
4. Wurzer A, DiCarlo D, Schmidt A, et al. Radiohybrid ligands: a novel tracer concept exemplified by ^{18}F- or ^{68}Ga-labeled rhPSMA-inhibitors. *J Nucl Med.* 2020; 61:735–742.
5. Eiber M, Kronke M, Wurzer A, et al. ^{18}F-rhPSMA-7 positron emission tomography for the detection of biochemical recurrence of prostate cancer following radical prostatectomy. *J Nucl Med.* 2020;61:696–701.
6. Kroenke M, Wurzer A, Schwamborn K, et al. Histologically-confirmed diagnostic efficacy of ^{18}F-rhPSMA-7 positron emission tomography for N-staging of patients with primary high risk prostate cancer. *J Nucl Med.* 2020;61:710–715.
7. Soeda F, Watabe T, Naka S, et al. Impact of ^{18}F-PSMA-1007 uptake in prostate cancer using different peptide concentrations: preclinical PET/CT study on mice. *J Nucl Med.* 2019;60:1594–1599.
8. Gafita A, Bieth M, Kronke M, et al. qPSMA: Semiautomatic software for whole-body tumor burden assessment in prostate cancer using ^{68}Ga-PSMA11 PET/CT. *J Nucl Med.* 2019;60:1277–1283.
9. Wurzer A, Pollmann J, Schmidt A, Reich D, Wester HJ, Notni J. Molar activity of Ga-68 labeled PSMA inhibitor conjugates determines PET imaging results. *Mol Pharm.* 2018;15:4296–4302.
10. Tolvanen T, Kalliokoski KK, Malaspina S, et al. Safety, biodistribution and radiation dosimetry of ^{18}F-rhPSMA-7.3 in healthy adult volunteers. *J Nucl Med.* 2021; 62:679–684.
11. Kalidindi TM, Lee SG, Jou K, et al. A simple strategy to reduce the salivary gland and kidney uptake of PSMA-targeting small molecule radiopharmaceuticals. *Eur J Nucl Med Mol Imaging.* 2021;48:2642–2651.
12. Kesch C, Kratochwil C, Mier W, Kopka K, Giesel FL. ^{68}Ga or ^{18}F for prostate cancer imaging? *J Nucl Med.* 2017;58:687–688.